JOURNAL OF AGRICULTURAL AND FOOD CHEMISTRY

Article

pubs.acs.org/JAFC

Structural Features of Copigmentation of Oenin with Different Polyphenol Copigments

Natércia Teixeira, Luís Cruz, Natércia F. Brás, Nuno Mateus, Maria João Ramos, and Victor de Freitas*

Centro de Investigação em Química, Departamento de Química e Bioquímica, Faculdade de Ciências, Universidade do Porto, Rua do Campo Alegre 687, 4169-007 Porto, Portugal

ABSTRACT: The copigmentation binding constants (K) for the interaction of different copigments with oenin (major red wine anthocyanin) were determined. All tests were performed in a 12% ethanol citrate buffer solution (0.2 M) at pH 3.5, with an ionic strength adjusted to 0.5 M by the addition of sodium chloride. Over the past years, several copigmentation studies were made and many copigments were tested, but none of them included prodelphinidin B3 or a dimeric-type adduct like oenin-(O)-catechin, probably due to the difficulty in obtaining them. The data yielded from this study allowed concluding that (a) the presence of a pyrogallol group in the B ring of the flavan-3-ol structure slightly increases the copimentation potential and (b) within all copigments tested oenin-(O)-catechin was revealed to be the best. According to computational studies performed on epicatechin/oenin, epigallocatechin/oenin, procyanidin B3/oenin, and oenin-(O)-catechin/oenin complexes, the $\Delta G_{binding}$ energy of the oenin-(O)-catechin/oenin complex is the most negative compared to the other copigmentation complexes, hence being more stable and thermodynamically favored. All structural data show that oenin-(O)-catechin and epigallocatechin are closer to the pigment molecule, which is in accordance with these two copigments having the highest experimental copigmentation binding constants for oenin.

KEYWORDS: *oenin-(O)-catechin, prodelphinidin B3, procyanidin B3, copigmentation binding constant*

INTRODUCTION

Anthocyanins are natural pigments widespread in the plant kingdom and are responsible for the colors of many flowers, fruits, and beverages such as red wine. It is well-known that the color exhibited by anthocyanins in aqueous solution is pH-dependent on the medium. At pH <2, the red flavylium cation is predominant and, as the pH increases, the other anthocyanin forms (hemiketal, chalcones, and quinonoidal bases) occur in equilibrium.[1] Taking into account that the pK_h of anthocyanins is between 2 and 3 in red wines (pH 3.2−4.0), it is expected that anthocyanins occur largely as colorless hemiketals in equilibrium with other forms (>70%). However, in nature, anthocyanins found some stabilizing mechanisms that allow them to exist mainly as flavylium cations and quinonoidal forms. Such mechanisms are described in the literature as resulting from noncovalent interactions of anthocyanins with themselves (self-association), with metal cations (metal complexation), with their own acylated residues (intramolecular copigmentation), and with other polyphenols (e.g., catechins and procyanidins) acting as copigments (intermolecular copigmentation).[2−7] The copigmentation phenomenon consists essentially of van der Waals interactions (vertical $\pi-\pi$ stacking) between the planar polarizable nuclei of the anthocyanin and the copigment. The anthocyanin/copigment complexes adopt a sandwich-like structure that stabilizes the flavylium cation chromophore (benzopyrylium) and partially protects it from the nucleophilic attack of water, thus preventing color loss.[8−10] Because flavonols generally have planar polyphenolic nucleus, they are excellent copigments that can interact with anthocyanins and protect them from water addition at C2 (the first step for anthocyanin discoloration),[11,12] whereas flavan-3-ols are comparatively weak copigments. According to the literature, flavan-3-ols do not have a good ability to act as copigments, probably due to their nonplanar structure, which does not allow close access to the anthocyanin.[13,14] Nevertheless, epicatechin is a better copigment than catechin[13,15] due to its B ring conformation, allowing it to be approximately coplanar; procyanidin dimers with C4−C6 interflavanic linkages seem to be better copigments that their respective C4−C8 dimers;[16] the presence of more hydroxyl groups [17] and galloylation at C3[16] increase the copigmentation effect.

Usually copigmentation produces an increase in absorbance (hyperchromic effect) and a positive shift of the wavelength of the visible absorption maximum (bathochromic effect). Besides the pigment and copigment molecular structure and their relative concentration, copigmentation was shown to be dependent on ionic strength, pH, solvent, temperature, and the presence of metal salts.[2,18−21]

The levels of polyphenols in red wines depend on the characteristics of the grape, environmental factors, and the winemaking process. In general, it is assumed that flavan-3-ols and anthocyanins are the major phenolic components in red wines. Red wine color evolution during aging and storage is in part attributed to copigmentation phenomena. These noncovalent interactions have been reported as the first step for the formation of covalent bonds between two molecules that result in new anthocyanin-derived pigments.[15,21,22] Indeed, during wine processing and aging, several chemical reactions involving

Received: March 15, 2013
Revised: May 28, 2013
Accepted: June 24, 2013
Published: June 24, 2013

dx.doi.org/10.1021/jf401174b | J. Agric. Food Chem. 2013, 61, 6942−6948

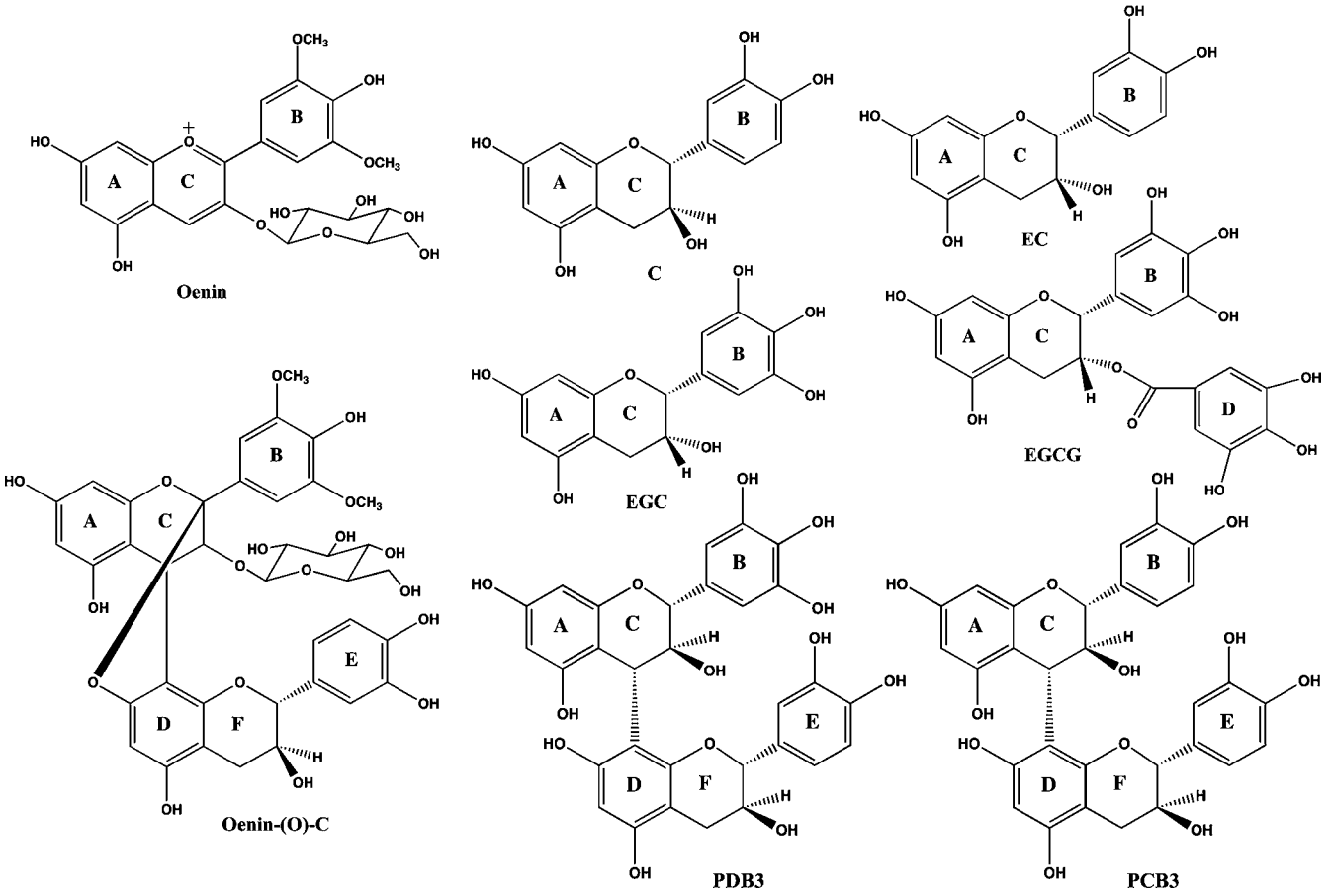

Figure 1. Chemical structures of the pigment (oenin) and copigments used.

anthocyanins, flavan-3-ols, and small molecules released by yeasts (e.g., pyruvic acid, acetaldehyde, acetoacetic acid, cinnamic acids) take place, yielding new families of anthocyanin-derived pigments, which will contribute to the modification of wine sensorial properties. Among them, direct and acetaldehyde-mediated condensations between anthocyanins and flavan-3-ols have been widely studied.[23−31] Direct reactions between anthocyanins and flavan-3-ols originate the dimeric-type flavanol-(4,8)-anthocyanin (F-A) and anthocyanin-(4,8)-flavanol (A-F) adducts. A-F adduct formation in red wines is described in the literature to arise from a nucleophilic attack of flavanols (C6/C8) to the electropositive C4 of anthocyanin, yielding a colorless product (flavene structure). This adduct could further evolve to the colorless bicyclic form (supplementary ether linkage type A, A-(O)-F) or undergo oxidation to give the red pigment A^+-F, which could dehydrate to the orange-yellow xanthylium salt.[29,32,33] Recently, the oenin-(O)-catechin dimeric adduct was hemisynthesized in model solution, isolated, and structurally characterized,[34] but its ability to act as a copigment with anthocyanins was never studied.

The aim of this work was to study the ability of different polyphenols present in red wine to act as copigments of oenin (the main anthocyanin of red wine) by determination of the respective copigmentation binding constants. The relationship between copigmentation ability and the structure of complexes was evaluated.

MATERIALS AND METHODS

Samples. Oenin was purchased from Extrasynthèse (France). (+)-Catechin (C) and (−)-epicatechin (EC) were purchased from Sigma-Aldrich (Madrid, Spain). (−)-Epigallocatechin (EGC) and (−)-epigallocatechin gallate (EGCG) were purchased from Biopurify Phytochemicals Ltd. (Sichuan, China). Procyanidin B3 (PCB3) and prodelphinidin B3 (PDB3) were extracted from barley according to the procedure described elsewhere.[35] These latter were isolated and purified by column chromatography (250 × 16 mm i.d.) in a TSK Toyopearl HW40(s) gel (Tosoh, Japan) column connected to an ultraviolet (UV) detector. The dimers were then repurified by semipreparative HPLC using an Elite LaChrom L-2130 quaternary pump and an Elite LaChrom L-2420 detector. The column used was a reversed-phase C18 column (250 × 4.6 mm i.d.), and the mobile phase was composed by solvent A, 2.5% (v/v) acetic acid, and solvent B, 20% (v/v) solvent A and 80% (v/v) acetonitrile. The flow rate was 1 mL/min, and the gradient method started with an isocratic gradient of 93% A during 5 min, followed by a linear gradient ranging from 93% A to 80% A in 90 min and a final isocratic gradient of 100% B during 10 min. The purified dimers were redissolved in water and freeze-dried for further use. The identity and purity of procyanidin B3 and prodelphinidin B3 were achieved by LC-MS-ESI (Finnigan Surveyor equipped with a Thermo Finnigan (Hypersil Gold) 150 mm × 4.6 mm, 5 μm, C18 reversed-phase column at 25 °C; a Finnigan LCQ DECA XP MAX mass detector (Finnigan Corp., San Jose, CA, USA) quadrupole ion trap equipped with an atmospheric pressure ionization source, using an electrospray ionization interface), and NMR (^{1}H NMR spectra were measured in D_2O on a Bruker Avance 400 spectrometer) by comparison with literature data.[35] Oenin-(O)-catechin (oenin-(O)-C) was obtained by hemisynthesis.[34] Briefly, a solution containing oenin (2.3 mM)/(+)-catechin (molar ratio of 1:20) was prepared in water (200 mL) at pH 2.5 (adjusted with dilute

dx.doi.org/10.1021/jf401174b | J. Agric. Food Chem. 2013, 61, 6942−6948

Table 1. Absorbance Values for the Oenin/Copigment Complexes at the Maximum Wavelength (λ_{max} 523 nm)

	oenin (10^{-4} M)						
	r = 0.953	r = 0.956	r = 0.897	r = 0.884	r = 0.958	r = 0.964	r = 0.891
pigment/copigment molar ratio	C	EC	EGC	EGCG	PDB3	PCB3	oenin-(O)-C
1:0 (A_0)	0.528	0.520	0.521	0.540	0.507	0.537	0.635
1:5	0.564	0.538	0.569	0.586	0.525	0.549	0.715
1:10	0.598	0.555	0.603	0.625	0.540	0.563	0.767
1:20	0.648	0.605	0.649	0.679	0.560	0.576	0.922
1:30	0.696	0.642	0.703	0.732	0.573	0.604	1.009
1:40	0.737	0.680	0.784	0.757	0.603	0.616	1.150

HCl or NaOH), protected from light/ and placed in the oven at 50 °C.

Copigmentation. All solutions used were prepared in a citrate buffer solution with 12% ethanol (0.2 M) at pH 3.5, and the ionic strength was adjusted to 0.5 M by addition of sodium chloride. Each pigment/copigment solution was prepared by mixing a volume of pigment solution (10^{-4} M) with an aliquot of copigment solution to give the required pigment/copigment molar ratio of 1:0, 1:5, 1:10, 1:20, 1:30, or 1:40. Each experiment was performed in triplicate. All of the solutions were left to equilibrate for 30 min before spectroscopic measurements. The absorbance values were collected at the maximum absorption wavelength of free oenin at pH 3.5 (λ_{max} 523 nm). Parameter r, which represents the ratio between the molar absorption coefficient of the complex (oenin/copigments molar ratio = 1:40) and the free flavylium ion (10^{-4} M), was determined in strongly acidic solutions (1 M aqueous HCl, pH ≈0) to ensure that flavylium ion is the sole anthocyanin form.

UV−Visible Spectroscopy. UV−visible spectra were recorded on a Bio-Tek Power Wave XS spectrophotometer at a constant temperature of 25 °C from 360 to 830 nm (1 nm sampling interval) using a 1 cm path length cell.

Data Analysis. The curve fittings were carried out on a PC using the Scientist program (MicroMath, Salt Lake City, UT, USA). Curve fittings were achieved through a least-squares regression method. Statistical analysis reported standard deviations and correlation coefficients.

Molecular Dynamic Simulations. The starting geometries of the copigment (EC, EGC, PCB3, and oenin-(O)-C) and pigment (oenin) molecules were obtained at the HF/6-31G(d) level of calculation, using the Gaussian 09 package.[36] Atomic charges were further recalculated using the RESP procedure.[37] MD simulations were performed with generalized amber force field (GAFF)[38] and the TIP3P model for the solute and water, respectively. Explicit solvation was included as a truncated octahedral box with a 12 Å distance between the box faces and any atom of the compounds. Energy minimization occurred in two stages: first, the solute was kept fixed, and only the positions of the water molecules and counterion were optimized (500 steps using the steepest descent algorithm and 1500 steps carried out using conjugate gradient); second, the full system was minimized (1000 steps using the steepest descent algorithm and 2000 steps carried out using conjugate gradient). Following a 100 ps equilibration procedure at constant volume and temperature, 30 ns MD simulations were carried out. The Langevin thermostat was used to control the temperature at 303.15 K,[39] and all of the simulations were carried out in the NPT ensemble with periodic boundary conditions. All MD simulations were carried out using the Sander module, implemented in the Amber 10.0 simulation package.[40] Bond lengths involving H-atoms were constrained using the SHAKE algorithm, and the equations of motion were integrated with a 2 fs time step using the Verlet leapfrog algorithm.[41] Nonbonded interactions were truncated with a 12 Å cutoff.

Calculation of Binding Free Energies. The MM_PBSA script (Molecular Mechanics−Poisson−Boltzmann Surface Area)[42−44] as implemented in the Amber 10.0 simulation package[40] was used to calculate the binding free energies ($\Delta G_{binding}$) for all complexes. A series of 150 geometries was extracted every 100 steps of each simulation. The internal energy (bond, angle, and dihedral) and the electrostatic and the van der Waals interactions were calculated using the Cornell force field[45] with no cutoff. The electrostatic solvation free energy was calculated by solving the Poisson−Boltzmann equation with the PBSA program, implemented in the Amber 10.0 simulation package.[40] The nonpolar contribution to the solvation free energy due to van der Waals interactions between the solute and the solvent and cavity formation was modeled as a term that is dependent on the solvent-accessible surface area of the molecule. As these compounds possess similar structures and binding modes, the relative binding energies ($\Delta\Delta G_{binding}$) were calculated with respect to the most stable complex.

RESULTS AND DISCUSSION

In this work, oenin (malvidin-3-*O*-*β*-D-glucoside) was mixed with increasing concentrations of different copigments, namely, C, EC, EGC, EGCG, PDB3, PCB3, and oenin-(O)-C (Figure 1), for a quantitative evaluation of the corresponding copigmentation complexes. No copigmentation studies had been performed with compounds with the oenin-(O)-C structure or with PDB3 due to the difficulty in obtaining them from natural sources.[46]

The intermolecular copigmentation studies were performed with a concentration of pigment of 1×10^{-4} M to minimize any self-association effects. It is known that ethanol largely reduces the copigmentation effect;[46] however, its inclusion in the experimental conditions attempts to mimic red wine composition. Also, previous copigmentation studies were attempted using only aqueous citrate buffer, but some copigments were found to be very difficult to dissolve properly and precipitated during the spectroscopic analysis. In weakly acidic conditions (pH 3.5), the flavylium and hemiketal forms are the anthocyanin predominant species (pK_h oenin = 2.70 ± 0.01).[47,48] The quinonoidal bases are present only to a very small extent[1] and can be neglected (first $pK_a \approx 4$).[1,49]

The copigmentation equilibrium is in competition with the hydration process; that is, the copigment molecule competes with water for the flavylium ion. With this in mind, the copigmentation binding constants (K) between oenin and the referred copigments could be evaluated from a general mathematical treatment that takes into account the thermodynamics of water addition onto the flavylium ion. Assuming a 1:1 stoichiometry for the complex and no complexation between the copigment and the colorless forms, the variations of visible absorbance A as a function of the total copigment concentration CP_t can be expressed as eq 1

$$A = \frac{A_0}{\frac{a}{r-a} + \frac{1}{(r-a)K} \times \frac{1}{CP_t}} + A_0 \quad (1)$$

where A_0 is the visible absorbance of the pigment in the absence of copigment, r is the ratio of the molar absorption

coefficient of the complex to that of the free flavylium ion, and $a = 1/1 + K_h \times 10^{pH}$.[48] The absorbance values obtained for the oenin/copigment complexes at the maximum absorption wavelength of free oenin at pH 3.5 (λ_{max} 523 nm) are presented in Table 1.

The absorbance increase with the copigment concentration reflects the preferential binding of the copigment to the flavylium ion and the subsequent shift of the hydration equilibrium toward the colored forms.

For each selected copigment, a plot of absorbance as a function of wavelength was performed and the typical behavior of copigmentation phenomena was observed: increase of absorbance (hyperchromic effect) and a slight batochromatic shift of λ_{max} as the copigment concentration increased. Figure 2

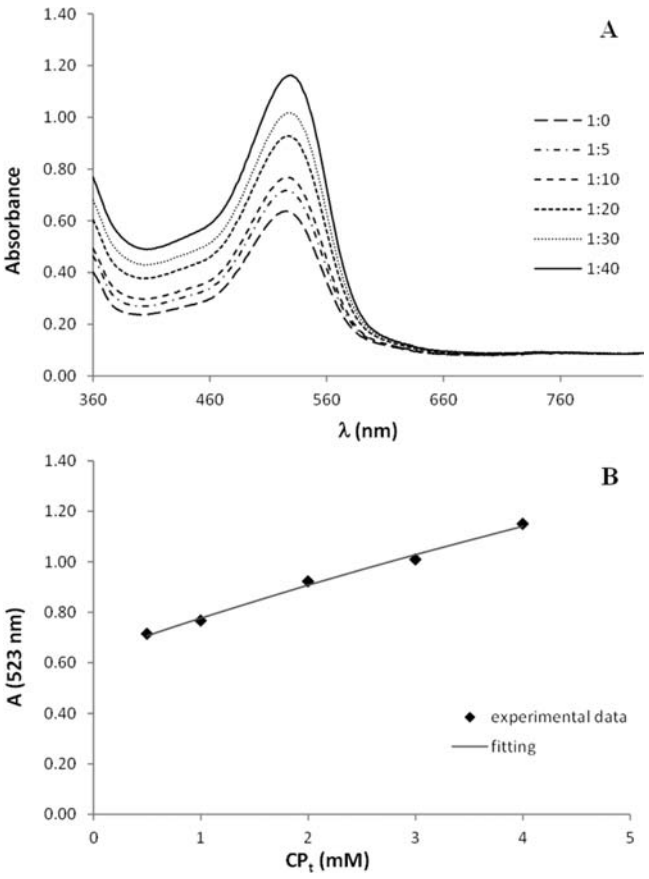

Figure 2. (A) Visible spectra of free oenin (1:0) and oenin/oenin-(O)-C solutions obtained at different molar ratios. (B) Plot of absorbance at 523 nm as a function of oenin-(O)-C concentration.

shows the absorption spectra of free oenin and oenin-(O)-catechin/oenin complex obtained at different molar ratios (A) and the respective mathematical treatment to determine K according to eq 1 (B).

Equation 1 was used for the curve fitting of $A = f(CP_t)$ to the experimental data to obtain the optimized values for K as the sole adjustable parameter. Statistical analysis gave good correlation coefficients and standard deviations for the copigmentation constants (K) (Table 2).

The experimental results show that all copigments have a r parameter close to 1 at 523 nm with the solution of the complex copigment/oenin showing a slight discoloration at pH ≈0 compared to oenin. Oenin-(O)-C was found to be the copigment with the highest copigmentation binding constant in

Table 2. Copigmentation Constants for the Oenin/Copigment Complexes

copigment	K^a (M^{-1})	R^2
C	136 (±4)	0.998
EC	99 (±2)	0.999
EGC	177 (±7)	0.992
EGCG	162 (±10)	0.991
PDB3	60 (±3)	0.991
PCB3	48 (±2)	0.992
oenin-(O)-C	309 (±7)	0.997

[a]Values in parentheses are the standard deviations of the curve-fitting procedure.

12% ethanol, pH 3.5, followed by EGC, EGCG, C, EC, PDB3, and PCB3. The highest value of K obtained for oenin-(O)-C is probably due to the existence of an extra glucose unit, allowing more hydrophobic interactions between glucose residue and the pigment rings. This results in the flavylium stabilization and prevents its hydration and consequent color loss.

The results obtained with EC, EGC, PDB3, and PCB3 showed that the presence of one more hydroxyl group in the B ring of the flavan-3-ol structure increases the copimentation potential. Futhermore, the presence of an additional OH group in ring B seems to be more efficient than the presence of a galloyl group, comparing the results for EC, EGC, and EGCG. Despite the fact that esterification of the C3 hydroxyl function by gallic acid adds a well-exposed planar $\pi-\pi$ stacking,[16] some steric hindrance may occur. This also can explain the lower K values obtained for dimers compared to monomers.

Under the conditions chosen for this work, catechin seems to more efficiently form copigment complexes with oenin than its isomer, epicatechin. To confirm and better explain these experimental results, some computational studies were performed.

Computational Studies of Four Pigment/Copigment Complexes. Molecular dynamics simulations were carried out for four distinct complexes, EC/oenin, EGC/oenin, PCB3/oenin, and oenin-(O)-C/oenin complexes, which allowed sampling of the potential hypersurface so as to identify several conformations for each copigmentation complex studied. The relative binding energies obtained by the MM_PBSA approach[42−44] are in relatively good agreement with the experimental results (Table 3), which confirms the relevance

Table 3. Relative Binding Free Energies of the Copigmentation Complexes

complex	theor $\Delta\Delta G_{binding}$ (kcal/mol)	exptl $\Delta\Delta G_{binding}$[a] (kcal/mol)
EC/oenin	2.73	0.85
EGC/oenin	0.14	0.51
PCB3/oenin	2.89	1.28
oenin-(O)-C/oenin	0.00	0.00

[a]Experimental values calculated from Table 2 using $\Delta\Delta G = RT \ln(K_{oenin\text{-}(O)\text{-}C}/K_{CPx})$.

of the MD procedure to provide an accurate picture for conformational analysis. It is noted that the theoretical $\Delta\Delta G_{binding}$ values fit only qualitatively with the experimental values, whereas the small quantitative differences could be due to some approximations within the MM_PBSA methodology. The results reveal that the $\Delta G_{binding}$ energy of the oenin-(O)-

dx.doi.org/10.1021/jf401174b | J. Agric. Food Chem. 2013, 61, 6942−6948

C/oenin complex is the most negative compared to the copigmentation complexes with EC, EGC, and PCB3. Therefore, the oenin-(O)-C/oenin complex displays higher stability and its formation is thermodynamically favored when compared to the other complexes. Although the tendency obtained for the binding free energies is oenin-(O)-C > EGC > EC > PCB3, the small differences in $\Delta\Delta G_{binding}$ between oenin-(O)-C and EGC, as well as EC and PCB3 (0.14 and 0.16 kcal/mol, respectively), reveal similar stabilities for the first two complexes and second two complexes.

Figure 3 shows the closest geometries to the average structures for the four copigment/oenin complexes. It is well-known that the formation of these complexes is driven by van der Waals interactions between the large planar surfaces of the pigment and copigment molecules and the concomitant release of high-energy water molecules from the solvation shells (hydrophobic effect). As this kind of copigmentation system has a large number of degrees of freedom, the steric hindrance does not allow optimized π-stacking arrangements. However, the binding could also be strengthened by H-bonding involving the numerous OH groups from glucose and phenolic units. Hence, the proximity between planar surfaces of the pigment and copigment molecules should reflect the stability of each complex. The interplanar distances between the benzopyrylium nucleus (AC), B ring, and glucose unit of the oenin and the aromatic and pyran rings of each copigment were calculated during each MD simulation. The minimal distances thus obtained are shown in Table 4. The results show that the AC rings of EGC and oenin-(O)-C are the closest planes to the benzopyrylium nucleous of oenin (4.34 and 4.92 Å, respectively). Furthermore, the AC plane of oenin-(O)-C and the B ring of EGC are the nearest planes to the B ring (4.76 and 4.33 Å, respectively). Although all copigment planes are very distant from the glucose residue, the minimal distances were obtained with the EGC and oenin-(O)-C molecules (6.76 and 6.86 Å, respectively). As the intermolecular distances of about 4 Å are consistent with van der Waals contacts, these data reveal that the shortest copigment/oenin distances were obtained for the complexes with the oenin-(O)-C and EGC copigments, which agrees with their highest stability constants (K).

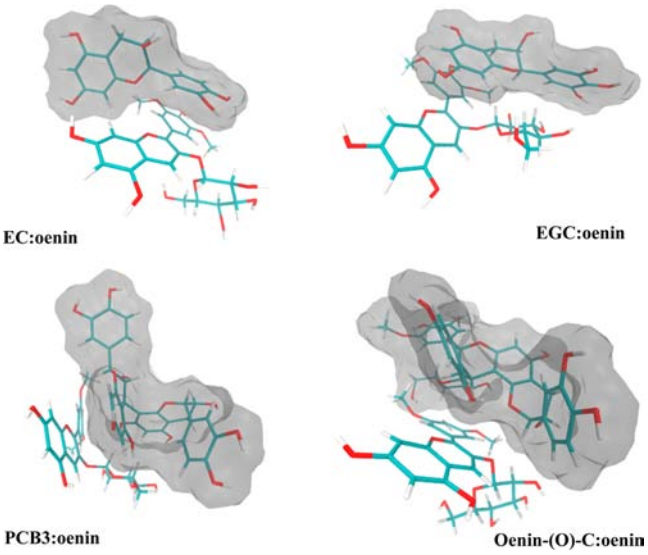

Figure 3. Closest geometries to the average structures of the EC/oenin, EGC/oenin, PCB3/oenin, and oenin-(O)-C/oenin complexes. Copigment structures are depicted with surface representation.

Table 4. Average Minimal Distances between Approximately Planar Surfaces of the Oenin and Copigment Molecules in the Copigmentation Complexes

	average minimal distance (Å)		
complex	benzopyrylium nucleus (AC)	B ring	Glc
EC/oenin	5.06 (AC)	5.35 (AC)	6.97 (B)
EGC/oenin	4.34 (AC)	4.76 (B)	6.76 (B)
PCB3/oenin	5.01 (AC)	5.53 (AC)	7.32 (AC)
oenin-(O)-C/oenin	4.92 (AC)	4.33 (AC)	6.86 (Glc)

Recently, the copigmentation between the 3-*O*-methylcyanidin and quercetin compounds was computationally studied by Meo et al.[50] According to their results, the contribution of copigmentation to color stability is dependent on the relative concentrations of pigment and copigment. It was verified that equal pigment and copigment concentrations result in complexes with high stability, which is the prevalent mechanism to avoid the hydration of the anthocyanin chromophore. The present results are in agreement with these data, and it was also verified that the driving force in the formation of copigmentation complexes appears to be dispersive interactions that greatly contribute to highly stable complexes and prevent the hydration of the pigment.

According to the structures of the four complexes shown in Figure 3, it was observed that oenin-(O)-C offers a very large planar surface for the establishment of multiple van der Waals interactions with the pigment. The untypical covalent interaction between the anthocyanin and catechin units observed in this copigment provides a huge roughly planar polarizable surface (AC-DF nucleus) that must be prone to strong π stacking interactions with the aromatic rings of oenin. In addition, it was observed that the benzopyrylium nucleus of EGC is strategically positioned in the middle of the pigment structure, establishing an accessible face and a closer contact with all planes of oenin. This fact contributes to a great binding of EGC and oenin molecules and thus to the also higher K values obtained for this complex.

For EC/oenin, it was observed that the AC nucleus of the copigment is perpendicularly located to the flavylium plane of oenin, which makes the establishment of nonpolar contacts between both molecules difficult. In relation to the PCB3/oenin complex, it was noted that EGC has its catechin unit facing opposite sides, which prevents a simultaneous interaction of both moieties with the flavylium nucleus of oenin. As the hydrophobic contacts with the flavylium nucleus of oenin are great contributions to the copigmentation driving force, it is expected that EC and PCB3 have the smallest copigmentation binding constants.

All of these structural data show that, within the complexes studied, oenin-(O)-C and EGC are closer to the pigment molecule than EC and PCB3. This is in accordance with their highest copigmentation binding constants calculated experimentally.

AUTHOR INFORMATION

Corresponding Author

*(V.F.) E-mail: vfreitas@fc.up.pt. Fax: +351 220 402 658 Phone: +351 220 402 558.

Funding

N.T., L.C., and N.F.B. gratefully acknowledge Ph.D. and Post Doctoral grants from FCT (SFRH/BD/70053/2010, SFRH/BPD/72652/2010, and SFRH/BPD/71000/2010, respectively).

Notes

The authors declare no competing financial interest.

■ ACKNOWLEDGMENTS

We thank Dra. Zélia Azevedo for the LC-DAD/ESI-MS analysis and Dra. Mariana Andrade for the NMR analysis.

■ REFERENCES

(1) Brouillard, R.; Delaporte, B. Chemistry of anthocyanin pigments. 2. Kinetic and thermodynamic study of proton-transfer, hydration, and tautomeric reactions of malvidin 3-glucoside. *J. Am. Chem. Soc.* **1977**, *99*, 8461−8468.

(2) Asen, S.; Stewart, R. N.; Norris, K. H. Copigmentation of anthocyanins in plant-tissues and its effect on color. *Phytochemistry* **1972**, *11*, 1139−1144.

(3) Boulton, R. The copigmentation of anthocyanins and its role in the color of red wine: a critical review. *Am. J. Enol. Vitic.* **2001**, *52*, 67−87.

(4) Dangles, O. Anthocyanin complexation and colour expression. *Analysis* **1997**, *25*, M50−M52.

(5) Goto, T.; Kondo, T. Structure and molecular stacking of anthocyanins − flower color variation. *Angew. Chem., Int. Ed.* **1991**, *30*, 17−33.

(6) Haslam, E. *Anthocyanin Copigmentation - Fruit and Floral Pigment*; Cambridge Press University: Cambridge, UK, 1998; pp 262−297.

(7) Robinson, G. M.; Robinson, R. A survey of anthocyanins. I. *Biochem. J.* **1931**, *25*, 1687−1705.

(8) Goto, T. Structure, stability and color variation of natural anthocyanins. *Prog. Chem. Org. Nat. Prod.* **1987**, *52*, 113−158.

(9) Goto, T.; Tamura, H.; Kawai, T.; Hoshino, T.; Harada, N.; Kondo, T. Chemistry of metalloanthocyanins. *Ann. N.Y. Acad. Sci.* **1986**, *471*, 155−173.

(10) Santos-Buelga, C.; De Freitas, V. Influence of phenolics on wine organoleptic properties. In *Wine Chemistry and Biochemistry*; Moreno-Arribas, M. V., Polo, C., Eds.; Springer: Berling, Germany, 2009; pp 529−570.

(11) Furtado, P.; Figueiredo, P.; Neves, H. C.; Pina, F. Photochemical and thermal degradation of anthocyanins. *J. Photochem. Photobiol. A* **1993**, *78*, 113−118.

(12) Cruz, L.; Brás, N. F.; Teixeira, N.; Mateus, N.; Ramos, M. J.; Dangles, O.; de Freitas, V. Vinylcatechin dimers are much better copigments for anthocyanins then catechin dimer procyanidin B3. *J. Agric. Food Chem.* **2010**, *58*, 3159−3166.

(13) Brouillard, R.; Wigand, M. C.; Dangles, O.; Cheminat, A. pH and solvent effects on the copigmentation reaction of malvin with polyphenols, purine and pyrimidine-derivatives. *J. Chem. Soc., Perkin Trans. 2* **1991**, *8*, 1235−1241.

(14) Gómez-Míguez, M.; González-Manzano, S.; Escribano-Bailón, M. T.; Heredia, F. J.; Santos-Buelga, C. Influence of different phenolic copigments on the color of malvidin 3-glucoside. *J. Agric. Food Chem.* **2006**, *54*, 5422−5429.

(15) Liao, H.; Cai, Y.; Haslam, E. Polyphenols interactions. Anthocyanins: copigmentation and colour changes in red wines. *J. Sci. Food Agric.* **1992**, *59*, 299−305.

(16) Berké, B.; de Freitas, V. A. P. Influence of procyanidin structures on their ability to complex with oenin. *Food Chem.* **2005**, *90*, 453−460.

(17) Chen, L. J.; Hrazdina, G. Structural aspects of anthocyanin-flavonoid complex-formation and its role in plant color. *Phytochemistry* **1981**, *20*, 297−303.

(18) Asen, S.; Stewart, R. N.; Norris, K. H. Co-pigmentation effect of quercetin glycosides on absorption characateristics of cyanidin glycosides and color of red wing azalea. *Phytochemistry* **1971**, *10*, 171−175.

(19) Asen, S.; Stewart, R. N.; Norris, K. H. Copigmentation of aurone and flavone from petals of antirrhinum-majus. *Phytochemistry* **1972**, *11*, 2739−2741.

(20) Mazza, G.; Brouillard, R. Polyphenol interations. Part 5 anthocyanin co-pigmentaion. *J. Chem. Soc., Perkin Trans.* **1990**, *2*, 1287−1296.

(21) Brouillard, R.; Dangles, O. Anthocyanin molecular interactions: the first step in the formation of new pigments during wine aging? *Food Chem.* **1994**, *51*, 365−371.

(22) Cai, Y.; Lilley, T. H.; Haslam, E. Polyphenol anthocyanin copigmentation. *J. Chem. Soc., Chem. Commun.* **1990**, 380−383.

(23) Dallas, C.; Ricardo-da-Silva, J. M.; Laureano, O. Products formed in model wine solutions involving anthocyanins, procyanidin B-2, and acetaldehyde. *J. Agric. Food Chem.* **1996**, *44*, 2402−2407.

(24) Es-Safi, N. E.; Fulcrand, H.; Cheynier, V.; Moutounet, M. Studies on the acetaldehyde-induced condensation of (−)-epicatechin and malvidin 3-*O*-glucoside in a model solution system. *J. Agric. Food Chem.* **1999**, *47*, 2096−2102.

(25) Rivas-Gonzalo, J. C.; Bravo-Haro, S.; Santos-Buelga, C. Detection of compounds formed through the reaction of malvidin-3-monoglucoside and catechin in the presence of acetaldehyde. *J. Agric. Food Chem.* **1995**, *43*, 1444−1449.

(26) Timberlake, C. F.; Bridle, P. Interactions between anthocyanins, phenolic compounds and acetaldehyde and their significance in red wines. *Am. J. Enol. Vitic.* **1976**, *27*, 97−105.

(27) Pissarra, J.; Mateus, N.; Rivas-Gonzalo, J. C.; Santos-Buelga, C.; De Freitas, V. Reaction between malvidin 3-glucoside and (+)-catechin in model solutions containing different aldehydes. *J. Food Sci.* **2003**, *68*, 476−481.

(28) Hayasaka, Y.; Kennedy, J. A. Mass spectrometric evidence for the formation of pigmented polymers in red wine. *Aust. J. Grape Wine Res.* **2003**, *9*, 210−220.

(29) Jurd, L. Review of polyphenol condensation reactions and their possible ocurrence in aging of wines. *Am. J. Enol. Vitic.* **1969**, *20*, 195−197.

(30) Remy, S.; Fulcrand, H.; Labarbe, B.; Cheynier, V.; Moutounet, M. First confirmation in red wine of products resulting from direct anthocyanin-tannin reactions. *J. Sci. Food Agric.* **2000**, *80*, 745−751.

(31) Somers, T. C. The polymeric nature of wine pigments. *Phytochemistry* **1971**, *10*, 2175−2186.

(32) Duenas, M.; Salas, E.; Cheynier, V.; Dangles, O.; Fulcrand, H. UV-visible spectroscopic investigation of the 8,8-methylmethine catechin-malvidin 3-glucoside pigments in aqueous solution: structural transformations and molecular complexation with chlorogenic acid. *J. Agric. Food Chem.* **2006**, *54*, 189−196.

(33) Remy-Tanneau, S.; Le Guerneve, C.; Meudec, E.; Cheynier, V. Characterization of a colorless anthocyanin-flavan-3-ol dimer containing both carbon-carbon and ether interflavanoid linkages by NMR and mass spectrometry. *J. Agric. Food Chem.* **2003**, *51*, 3592−3597.

(34) Cruz, L.; Mateus, N.; De Freitas, V. Identification by mass spectrometry of new compounds arising from the reactions involving malvidin-3-glucoside-(*O*)-catechin, catechin and malvidin-3-glucoside. *Rapid Commun. Mass Spectrom.* **2012**, *26*, 2123−2130.

(35) Dvorakova, M.; Moreira, M. M.; Dostalek, P.; Skulilova, Z.; Guido, L. F.; Barros, A. A. Characterization of monomeric and oligomeric flavan-3-ols from barley and malt by liquid chromatography-ultraviolet detection-electrospray ionization mass spectrometry. *J. Chromatogr., A* **2008**, *1189*, 398−405.

(36) Frisch, M. J.; Trucks, G. W.; Schlegel, H. B.; Scuseria, G. E.; Robb, M. A.; Cheeseman, J. R.; Scalmani, G.; Barone, V.; Mennucci, B.; Petersson, G. A.; Nakatsuji, H.; Caricato, M.; Li, X.; Hratchian, H. P.; Izmaylov, A. F.; Bloino, J.; Zheng, G.; Sonnenberg, J. L.; Hada, M.; Ehara, M.; Toyota, K.; Fukuda, R.; Hasegawa, J.; Ishida, M.; Nakajima, T.; Honda, Y.; Kitao, O.; Nakai, H.; Vreven, T.; Montgomery, J. A., Jr.; Peralta, J. E.; Ogliaro, F.; Bearpark, M.; Heyd, J. J.; Brothers, E.; Kudin, K. N.; Staroverov, V. N.; Kobayashi, R.; Normand, J.; Raghavachari, K.; Rendell, A.; Burant, J. C.; Iyengar, S. S.; Tomasi, J.; Cossi, M.; Rega,

N.; Millam, N. J.; Klene, M.; Knox, J. E.; Cross, J. B.; Bakken, V.; Adamo, C.; Jaramillo, J.; Gomperts, R.; Stratmann, R. E.; Yazyev, O.; Austin, A. J.; Cammi, R.; Pomelli, C.; Ochterski, J. W.; Martin, R. L.; Morokuma, K.; Zakrzewski, V. G.; Voth, G. A.; Salvador, P.; Dannenberg, J. J.; Dapprich, S.; Daniels, A. D.; Farkas, Ö.; Foresman, J. B.; Ortiz, J. V.; Cioslowski, J.; Fox, D. J. *Gaussian 09*; Gaussian, Inc.: Wallingford, CT, 2009.

(37) Bayly, C. I.; Cieplak, P.; Cornell, W. D.; Kollman, P. A. A well-behaved electrostatic potential based method using charge restraints for deriving atomic charges − the RESP model. *J. Phys. Chem. U.S.* **1993**, *97* (40), 10269−10280.

(38) Wang, J. M.; Wolf, R. M.; Caldwell, J. W.; Kollman, P. A.; Case, D. A. Development and testing of a general amber force field. *J. Comput. Chem.* **2004**, *25* (9), 1157−1174.

(39) Izaguirre, J. A.; Catarello, D. P.; Wozniak, J. M.; Skeel, R. D. Langevin stabilization of molecular dynamics. *J. Phys. Chem. U.S.* **2001**, *114* (5), 2090−2098.

(40) Case, D. A.; Darden, T. A.; Cheatham, T. E., III; Simmerling, C. L.; Wang, J.; Duke, R. E.; Luo, R.; Crowley, M.; Walker, R. C.; Zhang, W.; Merz, K. M.; Wang, B.; Hayik, S.; Roitberg, A.; Seabra, G.; Kolossváry, I.; Wong, K. F.; Paesani, F.; Vanicek, J.; Wu, X.; Brozell, S. R.; Steinbrecher, T.; Gohlke, H.; Yang, L.; Tan, C.; Mongan, J.; Hornak, V.; Cui, G.; Mathews, D. H.; Seetin, M. G.; Sagui, C.; Babin, V.; Kollman, P. A. *AMBER 10*; University of California: San Francisco, CA, 2008.

(41) Ryckaert, J. P.; Ciccotti, G.; Berendsen, H. J. C. Numerical-integration of Cartesian equations of motion of a system with constraints − molecular-dynamics of *n*-alkanes. *J. Comput. Phys.* **1977**, *23* (3), 327−341.

(42) Huo, S.; Massova, I.; Kollman, P. A. Computational alanine scanning of the 1:1 human growth hormone-receptor complex. *J. Comput. Chem.* **2002**, *23* (1), 15−27.

(43) Kollman, P. A.; Massova, I.; Reyes, C.; Kuhn, B.; Huo, S. H.; Chong, L.; Lee, M.; Lee, T.; Duan, Y.; Wang, W.; Donini, O.; Cieplak, P.; Srinivasan, J.; Case, D. A.; Cheatham, T. E. Calculating structures and free energies of complex molecules: combining molecular mechanics and continuum models. *Acc. Chem. Res.* **2000**, *33* (12), 889−897.

(44) Massova, I.; Kollman, P. A. Combined molecular mechanical and continuum solvent approach (MM-PBSA/GBSA) to predict ligand binding. *Perspect. Drug Discov.* **2000**, *18*, 113−135.

(45) Cornell, W. D.; Cieplak, P.; Bayly, C. I.; Gould, I. R.; Merz, K. M.; Ferguson, D. M.; Spellmeyer, D. C.; Fox, T.; Caldwell, J. W.; Kollman, P A. A 2nd generation force-field for the simulation of proteins, nucleic-acids, and organic-molecules. *J. Am. Chem. Soc.* **1995**, *117* (19), 5179−5197.

(46) Dangles, O.; Brouillard, R. Polyphenol interactions − the copigmentation case − thermodynamic data from temperature-variation and relaxation kinetics-medium effect. *Can. J. Chem.* **1992**, *70*, 2174−2189.

(47) Dangles, O.; Elhajji, H. Synthesis of 3-methoxy-flavylium and 3-(*β*-D-glucopyranosyloxy)flavylium ions − influence of the flavylium substitution pattern on the reactivity of anthocyanins in aqueous-solution. *Helv. Chim. Acta* **1994**, *77*, 1595−1610.

(48) Malien-Aubert, C.; Dangles, O.; Amiot, M. J. Influence of procyanidins on the color stability of oenin solutions. *J. Agric. Food Chem.* **2002**, *50*, 3299−3305.

(49) Macanita, A. L.; Moreira, P. F.; Lima, J. C.; Quina, F. H.; Yihwa, C.; Vautier-Giongo, C. Proton transfer in anthocyanins and related flavylium salts. Determination of ground-state rate constants with nanosecond laser flash photolysis. *J. Phys. Chem. A* **2002**, *106*, 1248−1255.

(50) Meo, F. D.; Garcia, J. C. S.; Dangles, O.; Trouillas, P. Highlights on anthocyanin pigmentation and copigmentation: a matter of flavonoid *π*-stacking complexation to be described by DFT-D. *J. Chem. Theory Comput.* **2012**, *8*, 2034−2043.